Science of the Total Environment 572 (2016) 1422–1430

Contents lists available at ScienceDirect

Science of the Total Environment

journal homepage: www.elsevier.com/locate/scitotenv

Effects of spatial heterogeneity in moisture content on the horizontal spread of peat fires

Nuria Prat-Guitart [a,*], Guillermo Rein [b], Rory M. Hadden [c], Claire M. Belcher [d], Jon M. Yearsley [a]

[a] School of Biology and Environmental Science, Earth Institute, University College Dublin, Dublin D4, Ireland
[b] Department of Mechanical Engineering, Imperial College London, London SW7 2AZ, UK
[c] School of Engineering, University of Edinburgh, Edinburgh EH9 3JL, UK
[d] wildFIRE Lab, Hatherly Laboratories, University of Exeter, Exeter EX4 4PS, UK

HIGHLIGHTS

- Local heterogeneity of peat moisture content affects smouldering spread.
- Fire temperatures and combustion duration are sensitive to peat moisture gradients.
- The moisture before a gradient affects few centimetres of spread into a wet peat.

GRAPHICAL ABSTRACT

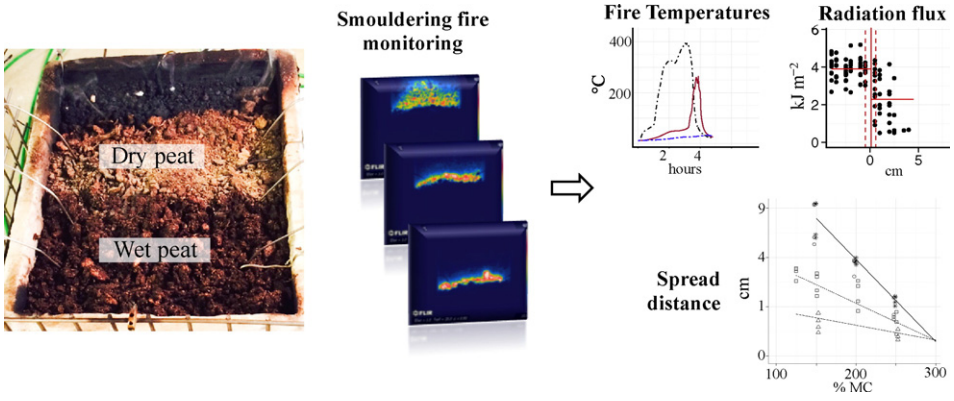

ARTICLE INFO

Article history:
Received 29 November 2015
Received in revised form 20 February 2016
Accepted 20 February 2016
Available online 20 April 2016

Keywords:
Peatland
Smouldering
Propagation
Breakpoint analysis
Step-change
Infrared image analysis

ABSTRACT

The gravimetric moisture content of peat is the main factor limiting the ignition and spread propagation of smouldering fires. Our aim is to use controlled laboratory experiments to better understand how the spread of smouldering fires is influenced in natural landscape conditions where the moisture content of the top peat layer is not homogeneous. In this paper, we study for the first time the spread of peat fires across a spatial matrix of two moisture contents (dry/wet) in the laboratory. The experiments were undertaken using an open-top insulated box (22 × 18 × 6 cm) filled with milled peat. The peat was ignited at one side of the box initiating smouldering and horizontal spread. Measurements of the peak temperature inside the peat, fire duration and longwave thermal radiation from the burning samples revealed important local changes of the smouldering behaviour in response to sharp gradients in moisture content. Both, peak temperatures and radiation in wetter peat (after the moisture gradient) were sensitive to the drier moisture condition (preceding the moisture gradient).
Drier peat conditions before the moisture gradient led to higher temperatures and higher radiation flux from the fire during the first 6 cm of horizontal spread into a wet peat patch. The total spread distance into a wet peat patch was affected by the moisture content gradient. We predicted that in most peat moisture gradients of relevance to natural ecosystems the fire self-extinguishes within the first 10 cm of horizontal spread into a wet peat patch. Spread distances of more than 10 cm are limited to wet peat patches below 160% moisture content (mass of

* Corresponding author.
E-mail address: prat.nur@gmail.com (N. Prat-Guitart).

http://dx.doi.org/10.1016/j.scitotenv.2016.02.145

water per mass of dry peat). We found that spatial gradients of moisture content have important local effects on the horizontal spread and should be considered in field and modelling studies.

1. Introduction

Peatland soils are significant reservoirs of carbon, they cover <3% of the Earth's land surface but they store 25% of the world's terrestrial carbon, approximately ~560 Gt of carbon (Turetsky et al., 2015; Yu, 2012). The drainage of peatlands for human activities combined with a lack of external water inputs (e.g. rain) perturbs peatland hydrological feedbacks (Waddington et al., 2015), leading to a suppression of the water table and drying of the surface peat. Enhanced drainage makes peatlands highly vulnerable to drying and subsequently fires (Turetsky et al., 2011). During flaming wildfires of the surface vegetation, part of the heat can be transferred to the organic soil (e.g. duff, peat) and may ignite a smouldering fire (Rein, 2013). These flameless fires are more difficult to detect and suppress than flaming vegetation fires (Rein, 2013). Peat fires can spread both on the surface and in-depth through the sub-surface of a peatland and can initiate new flaming fires well away from the initial region of smouldering peat (Putzeys et al., 2007; Rein, 2016). Very large amounts of peat can be consumed during smouldering fires, releasing carbon gases (e.g. CO_2, CO and CH_4) and other greenhouse gases to the atmosphere (Gorham, 1991; Turetsky et al., 2015). The 1997 Indonesian peat fires are estimated to have consumed approximately 3% of the soil carbon stock from Indonesia, ~0.95 Gt of carbon, which is equivalent to 15% of the global fossil fuels emissions for that year (Page et al., 2002). A 2007 peat fire event in the arctic tundra is estimated to have reduced 30% of the soil depth in the whole area studied and consumed 19% of the soil carbon stock of the region (Mack et al., 2011). The climate change projections forecast an increase in drought frequency and severity in many peatlands worldwide (Roulet et al., 1992), suggesting that peatlands will become more vulnerable to peat fires in the future (IPCC, Climate Change, 2013). This implies that larger amounts of carbon may be released to the atmosphere further contributing to the climate change and turning peatlands into carbon-sources rather than potential carbon sinks (Billett et al., 2010; Flannigan et al., 2009; Turetsky et al., 2002, 2015).

In peatlands, the physiochemical properties of the surface-unsaturated peat layers are influenced by the position of the water table and its associated hydrological responses (Waddington et al., 2015). Changes in water table position alter surface transpiration, evaporation and peat decomposition, which contribute to the moisture variability of the surface layers of peat (Waddington et al., 2015). The vegetation also plays a very important role in determining the moisture content distribution of the topmost peat layer. Hummock-forming *Sphagnum* mosses retain high levels of moisture in the whole peat profile (Hayward and Clymo, 1982; McCarter and Price, 2012). Other mosses (e.g. hollow *Sphagnum* species and feather mosses) do not have the same capacity to uptake water from the water table, depending more on the regularity of external water inputs (Thompson and Waddington, 2013). As a consequence, during drought periods *Sphagnum* hummocks remain wet while the surrounding peat becomes drier. The presence of vascular plants causes shading and interception of precipitation also affecting the surface transpiration and evaporation (Waddington et al., 2015). The rooting systems from trees are also a source of moisture spatial heterogeneity in the topmost peat layers (Rein et al., 2008). The combination of all these ecohydrological factors, specially during drought events, causes large moisture heterogeneity on the topmost layers of peatlands (Nungesser, 2003; Petrone et al., 2004).

The main factors governing the ignition and spread of smouldering are peat moisture content, organic content and bulk density (Frandsen, 1987, 1997; Reardon et al., 2007; Rein et al., 2008; Watts, 2012). Once peat is ignited, the fire is sustained by the energy released during the oxidation of the char (Hadden et al., 2013). This energy is dissipated, some being lost to the surroundings and some being transferred to drive the drying and pyrolysis of peat particles ahead of the oxidation front (Rein, 2016). If the energy produced is enough to overcome heat losses to the environment and preheat the surrounding peat, the smouldering front becomes self-propagating (Huang and Rein, 2014; Ohlemiller, 1985). The spread can be horizontal and vertical and the extent of smouldering in each direction depends largely on the conditions of the peat and the environment (Benscoter et al., 2011; Reardon et al., 2007; Rein, 2013). A vertically spreading smouldering front can penetrate a few meters into the soil (Rein, 2013). However, more often tends to be extinguished after a few centimetres as downward spread is limited by either the water table or the mineral soil layer (Benscoter et al., 2011; Huang and Rein, 2015; Zaccone et al., 2014). A smouldering front that spreads horizontally can contribute to consume a large area of dry peat soils above the water table. This kind of spread coupled with the spread of vegetation wildfires, often results in large surface areas being affected (Benscoter and Wieder, 2003; Shetler et al., 2008).

Previous studies have highlighted the importance of peat moisture content on the ignition and spread of peat fires (Frandsen, 1987; Huang and Rein, 2014, 2015; Lawson et al., 1997; Reardon et al., 2007). A 50% probability of ignition and early propagation has been estimated at 110–125% *MC*[1] (Frandsen, 1987; Huang and Rein, 2015; Rein et al., 2008). Recent experimental smouldering fires reveal horizontal spread rates between 1 and 9 cm h^{-1} in peats below 150% *MC* (Prat-Guitart et al., 2016). In peats with higher moisture content, between 150 and 200% *MC*, the smouldering is weak and self-extinguishes within the first 10 cm of the sample (Frandsen, 1997; Reardon et al., 2007).

Moisture content distributions of the topmost layer in peatlands are highly relevant to determining the spread of smouldering fires. Post peat-fire landscapes are often characterised by irregular peat consumption, were patches of peat associated with *Sphagnum* hummocks remain unburnt (Hudspith et al., 2014; Shetler et al., 2008; Terrier et al., 2014). Enhanced peat consumption has also been observed under trees, suggesting that fires spread through the peat adjacent to the roots (Davies et al., 2013; Miyanishi and Johnson, 2002). However, there is little understanding of how varying the peat moisture content (e.g. transition from feather moss to *Sphagnum*) across a spatial landscape affects the horizontal propagation of peat fires. This study experimentally examines the behaviour of a smouldering front as it propagates through a gradient of peat moisture content in order to (1) identify local changes in the fire behaviour associated with a transition of moisture content and (2) test whether the contiguous drier moisture content ahead of a transition affects the fire behaviour into a wet peat.

2. Materials and methods

2.1. Experimental system

In order to study the effect of a moisture content gradient on the smouldering spread behaviour we designed a simplified milled peat system that allows the natural sources of peat heterogeneity, such as moisture content, bulk density, mineral content and particle size to be

[1] Gravimetric moisture content is the mass of water per mass of dry peat expressed as a percentage.

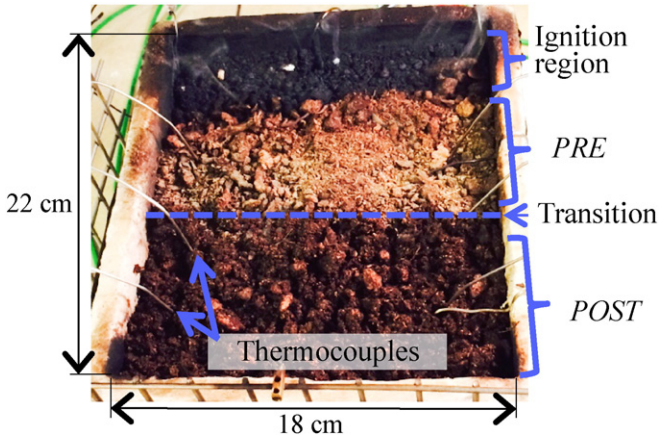

Fig. 1. Image of an on-going experimental burn. A glowing coil ignites the peat at the ignition region. The fire spreads through a region of *PRE* peat (dry peat) and then through a region of *POST* peat (wet peat). Dashed line indicates the location of the sharp gradient of moisture content between *PRE* and *POST* peat. Thermocouples monitor the temperatures inside the peat sample.

controlled (Prat-Guitart et al., 2015). The smouldering experiments were conducted in an 18 × 22 × 6 cm open-top box (insulated fibreboard container) of similar thermal conductivity as peat (0.07–0.11 W m^{-1} K^{-1}) to minimise boundary effects (Benscoter et al., 2011; Frandsen, 1987; Garlough and Keyes, 2011; Rein et al., 2008). The peat samples were 5 cm in depth. The samples were kept shallow to facilitate the formation of a plane smouldering front spreading horizontally from one side of the box to the other. As a result, we focus solely on the horizontally spread and not on the vertical spread. The experiments were limited to 12 h to avoid day-and-night temperature fluctuations.

The analysis of the spread inside the box was divided in three regions: (i) ignition region, (ii) region ahead of the moisture gradient (*PRE*) and (iii) region following the gradient (*POST*) (Fig. 1). The ignition region was at one side of the box where an 18-cm long electric igniter coil was buried in a 2-cm strip of peat at ~0% *MC*. The *PRE* region was adjacent to the ignition and consisted of a 10-cm strip of conditioned peat. The *POST* region was a peat sample of the same size as *PRE* but with higher moisture content. A clear straight boundary separated *PRE* and *POST* regions creating a sharp gradient in moisture content at approximately 10 cm from the ignition location.

The milled peat samples were oven-dried at 80 °C for 48 h and then rewetted in small samples of <300 g of peat to achieve the desired moisture content. Since oven-dried peats can become hydrophobic, rewetted peat samples were sealed in plastic bags for at least 24 h prior to the experiment to reach moisture equilibrium. One day is more than an order of magnitude longer than the typical infiltration time of severely hydrophobic soil (Kettridge and Waddington 2014). This protocol therefore minimises heterogeneity within the moisture content of the peat samples. We used 14 *PRE–POST* moisture content combinations in our experiment (Table 1). The *PRE* samples never exceeded 150% *MC* in order to be below the threshold of 125–150% *MC* for self-sustained spread for more than 10 cm (Frandsen, 1997; Prat-Guitart et al., 2016; Reardon et al., 2007). The moisture content of *POST* peats (between 125% and 250% *MC*) represents wet peats around the threshold of self-sustained spread. All peats had a mineral content[2] of 2.6 ± 0.2%. Within the box volume, peat bulk density (mass of dry peat per unit volume) varied between 55 and 140 kg m^{-3}. The variation in density was in part due to the expansion of peat when water was added (Table 1). Bulk densities were representative of peat soils from temperate and boreal peatlands (Davies et al., 2013; Lukenbach et al., 2015; Thompson and Waddington, 2013; Wellock et al., 2011).

The ignition protocol consisted in powering the ignition region with 100 W for 30 min using the electric igniter coil (Rein et al., 2008). This energy input is strong and similar to a burning tree stump and is enough to ignite dry peat (Rein et al., 2008). After 30 min the igniter coil was turned off and a linear smouldering combustion front spread through the samples of peat. A visual and infrared cameras imaged the surface of the smouldering every minute (Prat-Guitart et al., 2015). The infrared camera (SC640, FLIR Systems, US) captured the radiated energy flux from the peat at a resolution of 0.05 × 0.05 cm (i.e. one pixel equated to 0.25 mm^2). The images were corrected for the angle of the infrared and webcam cameras and processed to extract the values of radiated energy flux at a pixel scale. Details of the methods are given in Prat-Guitart et al. (2015). An array of seven K-type thermocouples (1.5 mm diameter) monitored the smouldering temperatures inside the peat samples at 1 cm from the bottom of the box. One thermocouple was situated in the ignition region and the other six were distributed to capture the temperature 4 cm before the moisture gradient and then at 1 and 6 cm after the moisture increase (Fig. 1).

2.2. Behaviour of the smouldering front

Smouldering temperatures have often been analysed to study the peat combustion and fire spread (Benscoter et al., 2011; Rein et al., 2008; Zaccone et al., 2014). We analysed the thermocouple data to identify changes in the combustion temperatures due to the sharp transition of peat moisture. For each thermocouple, we estimated the combustion duration, as the time taken since the start of the combustion (increase above 100 °C) and until the peat burnout (decreased below 200 °C for the last time). We also estimated the peak temperature as the 90th percentile of the thermocouple temperature profile. To demonstrate the effect of *PRE* moisture content on the spread into *POST* peats, we statistically compared the temperatures of 22 experiments with the same *POST* moisture content (150% *MC*) but different *PRE* moisture contents (25%–150% *MC*). The effects of moisture content treatment and distance from the moisture gradient on peak temperature and combustion duration were estimated using one-way ANOVAs. The differences between treatment levels were estimated using Tukey's Honesty Significant Difference (HSD) post-hoc test with a significance level of $p = 0.05$. Temperature profiles from all the *PRE–POST* combinations are provided in the supplementary materials (Fig. S1).

We also analysed the radiation flux from the smouldering of peat in order to identify changes in the smouldering behaviour due to the transition of moisture content. Even though the information from infrared imagery was limited to spread on the peat's surface, it allowed the smouldering spread to be monitored at a finer resolution than any array of thermocouples. We built a time-profile of each pixel's radiation flux (kW m^{-2}) and the radiation flux rate (kW m^{-2} min^{-1}) (Fig. 2). The start of the smouldering fire is defined by a peak in the radiation flux rate (Prat-Guitart et al., 2015). The last occurrence of a similar radiation flux value is used to define the end of the smouldering fire. From our defined start and end times of combustion we calculated the median radiated energy flux during combustion (*E*). Repeating this procedure for each pixel of the infrared box image gave a matrix of median radiation fluxes *E* during combustion.

We analysed the spatial autocorrelation of *E* by computing the data's semivariance (half average squared difference between pairs of pixels) (Bivand et al., 2008). The semivariogram was produced using a subset of *E* from each experimental burn. Subsets of *E* were selected from a central area of *PRE* peat away from any boundary. We then fitted a theoretical spherical model to the semivariogram. The spatial range of the semivariogram indicated the distance where the data exhibited no spatial autocorrelation. To avoid statistical issues of spatial autocorrelation we considered 48 sub-regions (2 × 1 cm) from each box and ensured that sub-regions were separated by at least 1 cm. This separation is

[2] Mass of mineral particles per mass of dry organic peat.

Table 1
Peat moisture content and bulk density combinations of the experimental burns. *PRE* and *POST* are the moisture contents of the two peat blocks before and after the sharp moisture gradient, respectively; peat bulk density (ρ) is the mass of dry peat per unit volume (median ± median absolute deviation); wet density is the mass of moist peat per unit volume and volumetric moisture content is the volume of water per unit volume. Number of experimental burn replicates (n) for each combination of *PRE* and *POST* moisture contents.

MC		ρ		Wet density		Volumetric *MC*		n
PRE	*POST*	*PRE*	*POST*	*PRE*	*POST*	*PRE*	*POST*	
(%)	(%)	(kg m^{-3})	(kg m^{-3})	(kg m^{-3})	(kg m^{-3})	(m^3 m^{-3})	(m^3 m^{-3})	
25	150	123 ± 6	65 ± 6	154 ± 7	163 ± 16	3.1 ± 0.1	9.8 ± 0.9	4
25	200	121 ± 10	66 ± 2	152 ± 12	199 ± 6	3.0 ± 0.2	13.2 ± 0.4	4
25	250	121 ± 7	75 ± 9	151 ± 9	263 ± 33	3.0 ± 0.2	18.8 ± 2.3	4
50	100	100 ± 2	84 ± 2	149 ± 3	167 ± 4	5.0 ± 0.1	8.4 ± 0.2	4
50	150	101 ± 3	69 ± 7	152 ± 4	173 ± 16	5.0 ± 0.1	10.4 ± 1.0	4
50	200	100 ± 6	70 ± 1	149 ± 10	210 ± 3	5.0 ± 0.3	14.0 ± 0.2	4
50	250	99 ± 2	70 ± 7	148 ± 4	244 ± 26	5.0 ± 0.1	17.4 ± 1.8	4
100	125	63 ± 3	64 ± 1	127 ± 6	144 ± 1	6.3 ± 0.3	8.0 ± 0.1	4
100	150	77 ± 6	73 ± 4	154 ± 12	184 ± 2	7.7 ± 0.6	11.0 ± 0.1	4
100	200	84 ± 2	70 ± 2	167 ± 6	212 ± 2	8.3 ± 0.2	14.1 ± 0.2	4
100	250	78 ± 2	73 ± 8	157 ± 4	254 ± 29	7.8 ± 0.2	18.1 ± 2.1	4
125	150	63 ± 2	69 ± 5	143 ± 4	173 ± 11	7.9 ± 0.2	10.4 ± 0.7	4
125	250	59 ± 2	68 ± 8	134 ± 5	238 ± 29	7.4 ± 0.7	17.0 ± 2.0	4
150	150	62 ± 4	62 ± 4	154 ± 10	154 ± 10	9.3 ± 0.7	9.3 ± 0.7	4

greater than the scale of autocorrelation in the data for E. We estimated the median E in each sub-region (E_m) and the median absolute deviation.

Piecewise linear regression was used to identify a step-change in E_m as a function of distance from the moisture gradient (Crawley, 2013). The analysis was performed on data from each moisture combination (i) separately as

$$E_{mi} = \beta_{d1}(x_i<c_i) + \beta_{d2}(x_i>c_i) \quad (1)$$

where x_i is the distance (cm) from the moisture gradient, c_i is the position of the breakpoint, β_{d1} and β_{d2} are the estimated intercepts before and after the breakpoint. To estimate the position of the breakpoint, Eq. (1) was fitted for values of c_i ranging from −4 cm to +8 cm in steps of 0.1 cm, and the values of c_i that produced the minimum residual standard error was selected.

2.3. Spread distance after a moisture gradient

The spread distance was estimated from the first visual image taken after the fire had extinguished (assessed with the infrared images). We used the visual images to distinguish by eye between the burnt and unburnt peat based on the colour; white and grey for the char and ash and brown for the unburnt peat (Fig. 1). We estimated the final position of the smouldering front into *POST* peat using the boundary between burnt and unburnt peat regions (often of irregular shape). The median spread distance after the moisture gradient (D_T) was estimated by manually removing the areas where fresh peat had collapsed. We associated D_T with the moisture content of *PRE* and *POST* peats using the following statistical model

$$\sqrt{(D_T)_i} = \beta_0 + \beta_1 PRE_i + \beta_2 POST_i + \beta_3 PRE_i{\cdot}POST_i + \varepsilon_i \quad (2)$$

where β_0, β_1, β_2 and β_3 are regression coefficients and ε_i are normally distributed residuals of the ith experimental replicate of each *PRE* and *POST* combination. The dependent variable (D_T) was square root transformed to normalise the distribution of the residuals. Experiments where the smouldering front completely consumed the *POST* sample (i.e. extinguished due to the box wall) were discarded since it was not possible to quantify D_T.

The image processing was done in Matlab with the *Image Processing Toolbox* (*Mathworks*, *version R2012b 8.0.0.783*). The data analysis was done with *R project* statistical software (Developement Core Team, 2013). The spatial autocorrelation analysis was done with packages *automap* (Hiemstra et al., 2009) and *gstat* (Pebesma, 2004).

3. Results

3.1. Smouldering behaviour

In experiments combining *PRE MC* of 25% and *POST* of 150% a breakpoint in E_m was identified at c_i = 1.5 cm after the moisture gradient (Table 2). The E_m before the breakpoint was 3.92 ± 0.05 kW m^{-2} (mean ± standard error), whereas after the breakpoint it decreased to

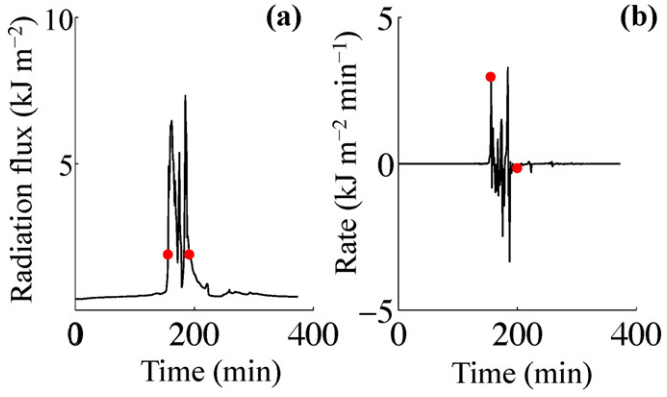

Fig. 2. Smouldering fire detection in radiation flux from infrared images. a) Time-profile of a pixel's radiation flux. b) Time-profile of the pixel's rate of radiation flux. Red dots indicate start and end of the smouldering fire.

Table 2
Location of the breakpoint and the median energy flux (E_m) estimated before and after the breakpoint. All results are for a moisture content *POST* = 150% *MC*. Breakpoint is the location (c_i, relative to the moisture gradient) of a breakpoint in E_m estimated using piecewise linear regression (Eq. (1)). CI is the breakpoint location's 95% confidence interval. 'E_m before' is E_m before the breakpoint (mean ± standard error), 'E_m after' is the E_m after the breakpoint.

PRE	Breakpoint	CI	E_m before	E_m after
(% *MC*)	(cm)	(cm)	(kW m^{-2})	(kW m^{-2})
25	1.5	1.0, 2.1	3.92 ± 0.05	2.89 ± 0.12
50	0.8	0.5, 1.1	3.03 ± 0.03	2.90 ± 0.07
100	1.5	1.0, 2.1	2.86 ± 0.08	2.13 ± 0.17
125	0.8	0.5, 1.1	2.78 ± 0.11	1.59 ± 0.26
150	−1.5	−2.0, −0.9	3.13 ± 0.09	2.33 ± 0.11

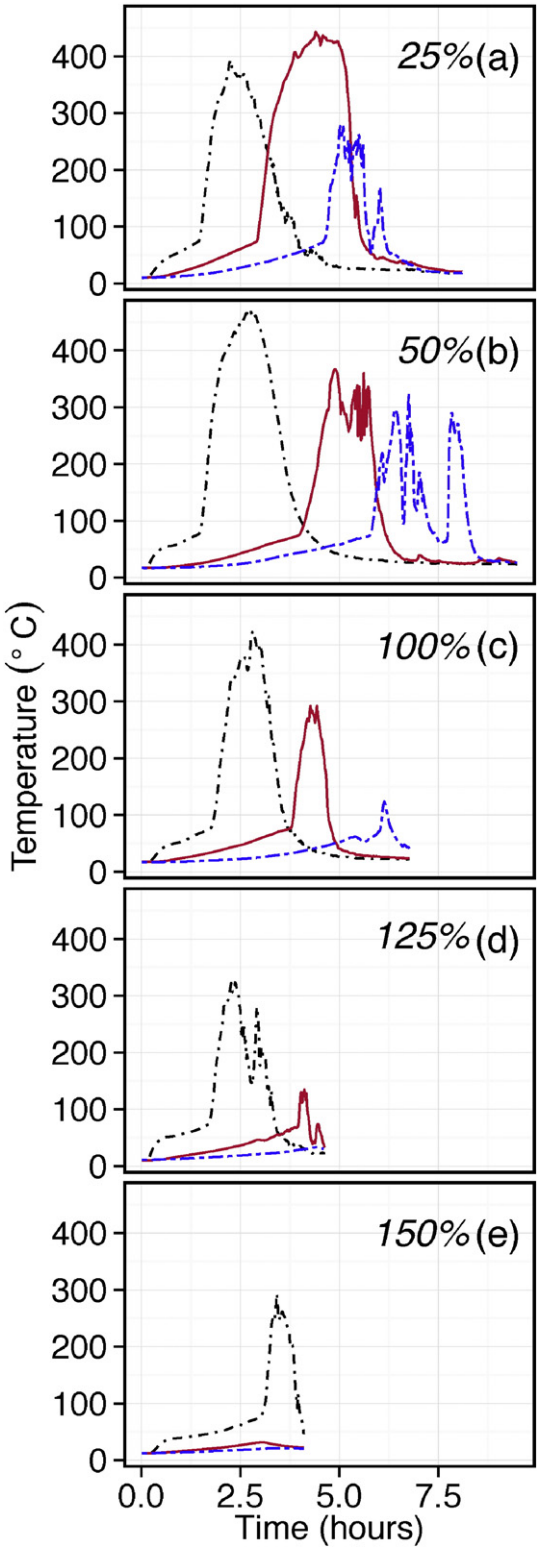

Fig. 3. Examples of temperature versus time profiles from five experiments (a–e). All experimental burns had *POST* peat moisture content of 150% and *PRE* peat moisture content of (a) 25%, (b) 50%, (c) 100%, (d) 125% and (e) 150%. Dot dash-black, solid red and double dash-blue lines correspond to thermocouples −4 cm, +1 cm and +6 cm from the moisture gradient, respectively. Profiles end when the fire self-extinguished.

2.89 ± 0.12 kW m^{-2}. In the experiments with *PRE MC* of 25% and *POST* of 150%, we found that the distance from the moisture content gradient was associated with differences in the peak temperature (one-way ANOVA $F_{2,16} = 11.1$, $p < 0.001$). Before the E_m breakpoint (at −4 cm and +1 cm from the moisture gradient) no difference in the peak temperatures was found (384 ± 25 °C and 349 ± 24 °C, respectively; Fig. 3a). However, the peak temperature at +6 cm from the moisture gradient (155 ± 93 °C) was less than peak temperatures before the breakpoint (Tukey's HSD $p < 0.05$). The combustion durations (113 ± 11 min, 107 ± 10 min and 56 min at −4 cm, +1 and +6 cm, respectively) were not associated with the distance from the moisture gradient (one-way ANOVA $F_{2,16} = 1.6$, $p = 0.2$).

At +1 cm from the moisture gradient both combustion duration and peak temperatures were affected by the *PRE* moisture contents (red lines in Fig. 3). We found that *PRE MC* was associated with peak temperatures at +1 cm (one-way ANOVA $F_{4,25} = 6.6$ $p < 0.001$). Peak temperatures did not differ between *PRE MC* of 25% and 50%, (349 ± 24 °C, 329 ± 21 °C, respectively), but a higher *PRE* moisture content significantly decreased the peak temperatures (e.g. 137 ± 27 °C in *PRE* = 150% *MC*) (Tukey's HSD $p < 0.05$). The combustion duration differed across *PRE MC* treatments (one-way ANOVA $F_{3,19} = 4.3$ $p = 0.02$). The combustion duration was similar for *PRE MC* of 25% and 50% (107 ± 10 min and 99 ± 18 min, respectively) but at higher *PRE* moisture contents (100%, 125% and 150% *MC*) the combustion duration decreased to 43 ± 5 min, 81 ± 9 min and 78 ± 9 min respectively (Tukey's HSD $p < 0.05$). At +6 cm from the moisture gradient (blue lines in Fig. 3) the combustion duration and peak temperatures were not different from to the ones reported for *PRE MC* of 150% (one-way ANOVAs $F_{3,7} = 1.1$ $p = 0.4$, $F_{2,3} = 0.65$ $p = 0.5$, respectively).

The finer resolution of the radiated energy flux data (E_m) added information on the location where the changes in fire behaviour took place (Table 2, Fig. 4, Fig. S2). The majority of breakpoints in E_m were located after the increase of moisture content, indicating a continuation of *PRE*-moisture gradient behaviour for up to 6 cm into the *POST* peat. Two moisture content combinations (*PRE* = 150%, *POST* = 150% and *PRE* = 125%, *POST* = 250%) had breakpoints in E_m before the moisture gradient (Table 2, Fig. S2).

3.2. Spread distance into wet peat

The spread distance (D_T) showed no difference between *PRE* of 25% and 50% *MC* (ANOVA $F_{1,22} = 0.067$ $p = 0.8$) (Fig. 5). For all other peat combinations, the smouldering front spread no further than 5 cm into the wetter peat ($D_T < 5$ cm). Experiments that combined *PRE MC* of 125% or *POST MC* of 250% *MC* always had self-extinction < 1 cm after the moisture transition.

The spread distance into wet peat was well described by *PRE* and *POST* moisture content conditions (Table 3, Fig. 6). Increasing either *PRE* or *POST* moisture contents decreased the spread distance. The coefficient β_1 was higher (−0.06, −0.04, 95% confidence interval) than β_2 (−0.03, −0.02), indicating a bigger effect of *PRE* moisture content on D_T than *POST* moisture content. The interaction term *PRE* × *POST* showed that the effect of *PRE* on reducing the spread distance was larger when *POST* peats had lower moisture content.

PRE MC above 125% lead to smouldering self-extinction immediately after the transition (<1 cm) for any *POST MC* (Fig. 7). Similarly, high *POST MC* (>260% *MC*) spreads for <1 cm for any *PRE MC*. Eq. (2) predicts that spread for more than 10 cm can be achieved when most *PRE MC* is below 50% combined with *POST MC* below 160%.

4. Discussion

4.1. Effects of peat moisture content heterogeneity on the propagation dynamics

We have analysed the behaviour of smouldering fires through a gradient in peat moisture. We find that the peat moisture before the gradient influences the fire spread into the wet peat beyond. The smouldering ignition and spread in peats with homogeneous moisture

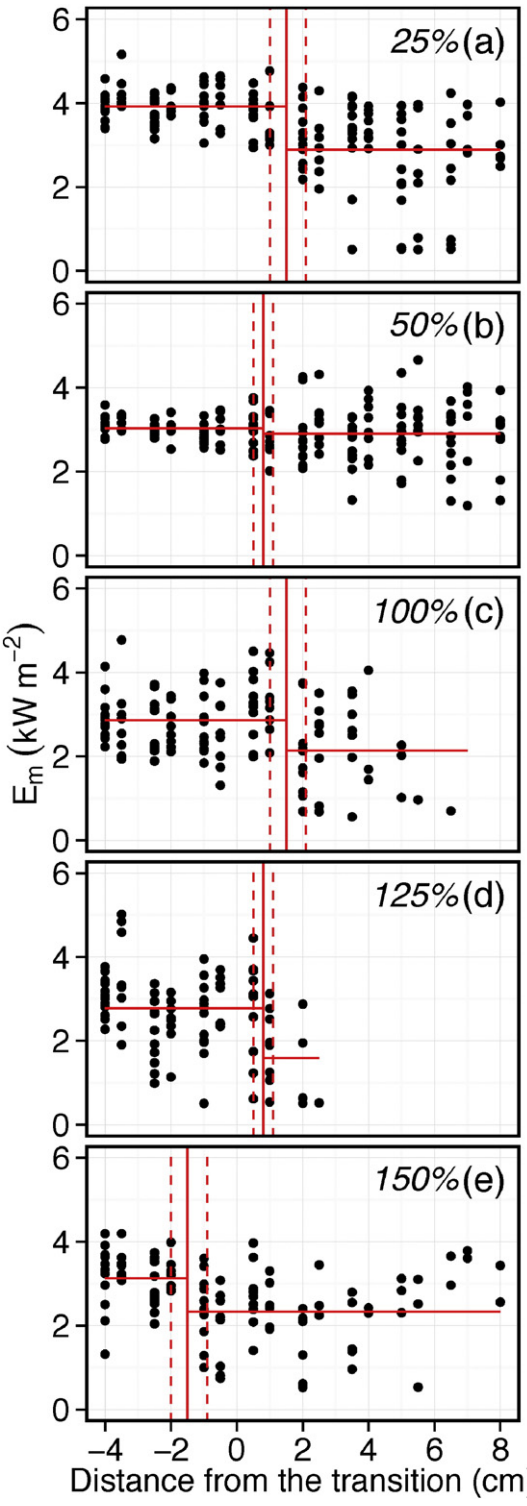

Fig. 4. Median radiation flux during smouldering combustion (E_m) as a function of distance from the moisture gradient. Data are for moisture contents of *POST* = 150% *MC* and *PRE*s of (a) 25%, (b) 50%, (c) 100%, (d) 125% and (e) 150% *MC*. Solid vertical red line indicates location of a breakpoint in E_m (Table 2) and dashed red lines the 95% confidence interval. Solid horizontal red lines are the E_m means over the four experiment replicates estimated using Eq. (1).

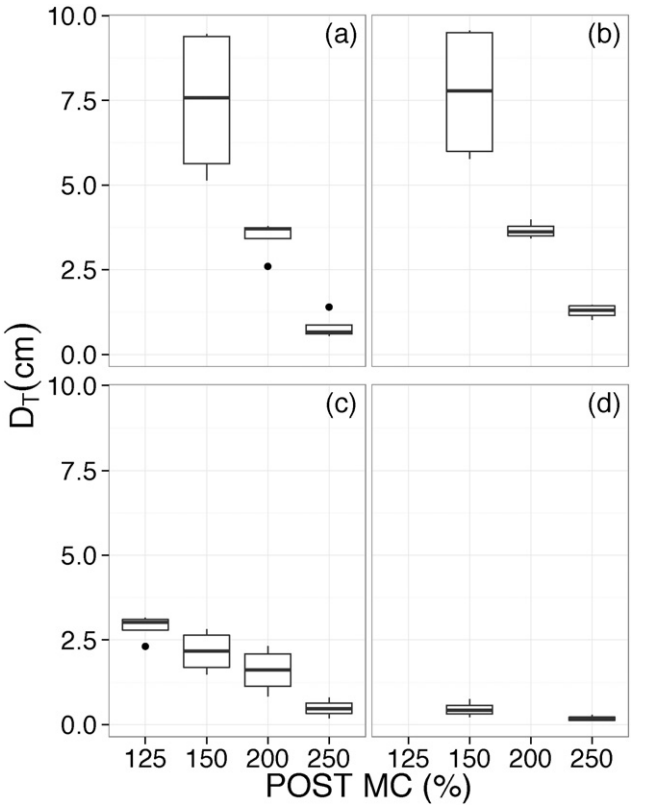

Fig. 5. Observations of spread distance (D_T) into *POST* peat. Subplots are for *PRE* peats of (a) 25%, (b) 50%, (c) 100% and (d) 125% *MC*.

conditions are primarily limited by the moisture content of the peat (Frandsen, 1987, 1997; Garlough and Keyes, 2011; Lawson et al., 1997; Reardon et al., 2007). However, we show that fire spread in milled peats with heterogeneous moisture conditions is strongly influenced by the moisture conditions of adjacent peat as well as the immediate moisture content of the peat.

Whilst, this study reports limited spread distances of 10 cm into a more moist peat, the scale of the experiment was enough to examine local changes in fire behaviour during the spread through a moisture gradient. Our analysis of radiation flux suggests two main effects of the *PRE* peat conditions on the fire behaviour after a moisture gradient. First, the strongest effect of *PRE* peat conditions happens within the first centimetres (<7 cm) after the moisture gradient (Fig. 4, Fig. S2). In this region the combustion duration and the peak smouldering temperatures have similar behaviour to the adjacent drier peat. The smouldering front spreading close to the moisture gradient evaporates part of the water from the wet peat (Ohlemiller, 1985). Consequently, a few centimetres ahead of the moisture gradient are already drier when the smouldering front reaches the wetter *POST* peat. Second, the location of the breakpoint could be interpreted as a new moisture gradient created by the dynamics of the smouldering fire. After the breakpoint the smouldering fire continues spreading but is less affected by the *PRE MC* conditions (Fig. 4). Experiments with *PRE* = 50% and *POST* = 150% did not have a substantial change in E_m after the breakpoint but an increase of the standard error of the E_m after (Table 2). We tested

Table 3
Coefficient estimates from the model of spread distance (D_T) after a peat moisture gradient. Dependent variable D_T was square-root transformed. Coefficients β_1, β_2 and β_3 are parameter estimates for *PRE* and *POST* moisture gradient and their interaction, respectively. $R^2 = 0.92$, residual standard error = 0.21.

	Coefficient (cm$^{0.5}$)	Standard error (cm$^{0.5}$)	p-Value
β_0, intercept	8.0	0.6	<0.0001
β_1, PRE_i	−0.054	0.006	<0.0001
β_2, $POST_i$	−0.026	0.003	<0.0001
β_3, $PRE_i \times POST_i$	0.00018	0.00003	<0.0001

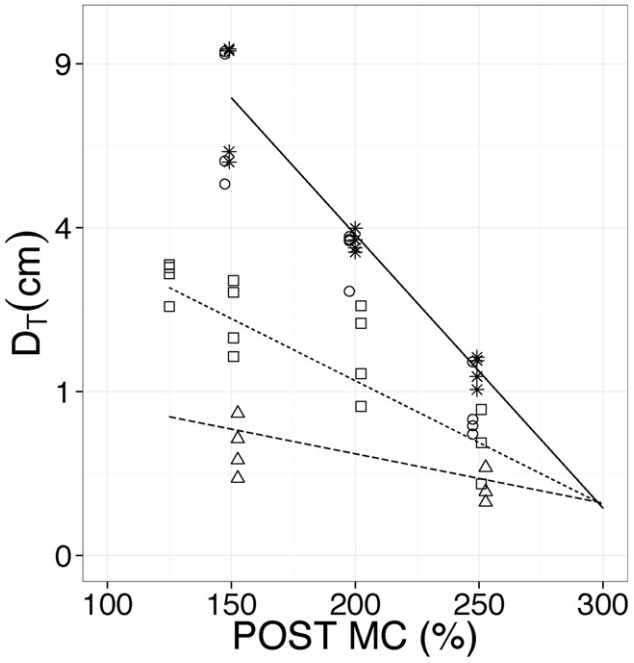

Fig. 6. Spread distance (D_T) as function of *POST* moisture gradient. Symbols represent experimental observations for *PRE* conditions, circle = 25%, star = 50%, square = 100%, triangle = 125% *MC*. Lines are model predictions from the coefficients in Table 3.

the sensitivity of the results obtained to changes in the methods used to analyse the infrared images. Variation of the thresholds used to determine *E* produced different *E* and E_m outputs, although the results did not change qualitatively.

The analysis of thermocouple temperature data also supports the effect of *PRE* peat conditions on the smouldering spread into *POST* peat. While the temperatures measured at 1 cm after the moisture gradient correspond to the region of *POST* peat more affected by the *PRE MC* conditions, the temperatures recorded at 6 cm after the moisture gradient were less affected by the *PRE* peat conditions (Fig. 4). We found that *POST MC* of 150% reach temperatures between 100 and 500 °C at 1 cm after the moisture gradient. Some of these temperatures are lower than typical oxidation temperatures 400–600 °C reported for natural peats ≤ 100% *MC* (Benscoter et al., 2011; Rein et al., 2008). Only

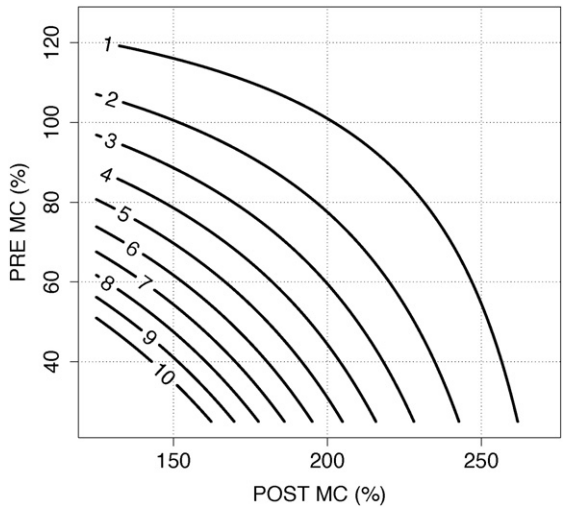

Fig. 7. Predicted spread distance (cm) into a wet peat for a range of *PRE* and *POST* moisture content combinations using the model in Table 3.

temperatures above 300 °C indicate on-going peat oxidation (Chen et al., 2011). Between 100 °C and 300 °C evaporation and pyrolysis processes dominate the smouldering and little oxidation is expected (Huang and Rein, 2014). Compared to the infrared images, the resolution of thermocouple data are limited and only providing data from fire behaviour around the thermocouple. In some burns, the thermocouples registered oscillations in combustion temperatures between 50 and 300 °C (i.e. Fig. 3a and b), which could be caused by the local dynamics of the particles surrounding the thermocouple. The milled peat particle size was below 1 cm in diameter and had variable density due to differences in the degree of decomposition. Differences in the infiltration rates and hydrophobicity of the peat particles during the rewetting process (Kettridge and Waddington 2014) could cause short-term heterogeneity (~10 min) in the moisture content of a peat sample. This short-term heterogeneity was minimised by our protocol, which allowed samples to equilibrate for 24 h prior to an experiment. Any remaining variation in peat moisture will impact the fine-scale spread of the fire between particles (i.e. <1 cm), but have a minor effect on the average spread of the fire throughout a peat sample of 20 × 20 cm.

The moisture gradient between *PRE* and *POST* peat could cause movement of the water through the transition boundary. Higher moisture content in *POST* peat could move to *PRE* peat, due to differences in unsaturated hydraulic conductivity (capacity of water movement in unsaturated soil per unit volume) (Boelter, 1965; Hillel, 1980). Milled peats below 250% *MC* have a small unsaturated hydraulic conductivity and therefore very little water movement is expected for the duration of the experimental burns (Holden and Ward, 1997). The smouldering fronts reached *POST* peat < 4 h after ignition implying minimal water movement during that time. Only peat samples with *PRE* of 125% and *POST* 250% and homogeneous 150% *MC* had a breakpoint in E_m before the moisture gradient (Fig. S2). This breakpoint before the initial location of the gradient could be caused by a weak smouldering spread due to the high moisture content in those *PRE* peat. Even after several hours, little moisture evaporation is expected for peat moisture contents below 250% *MC* (Kettridge et al., 2012). Our data (Prat-Guitart et al., 2016) confirm that there is little change in peat moisture content after 12 h at ambient temperature. Movement of water is therefore mainly due to evaporation and condensation ahead of the smouldering front, which is driven by the oxidative combustion reactions (Rein, 2016).

The spread distance into a wet peat is also affected by local changes in fire behaviour caused by the moisture gradient. The moisture content conditions of *PRE* peat conditions control the fire spread during the first 10 cm into a wet peat (Table 3). Only *PRE MC* of 25 or 50% combined with *POST MC* of 100 or 150% and few homogeneous peats with 150% *MC* led to peat fires that could propagate more than 10 cm. The fire behaviour found for these moisture content combinations agrees with results from previous studies indicating self-sustained spread for 10 cm or more in similar moisture conditions (Frandsen, 1997; Prat-Guitart et al., 2015; Reardon et al., 2007; Rein et al., 2008).

Our simplified laboratory experiments enabled the effect of moisture content on the spread of smouldering fires to be studied whilst controlling for mineral content, bulk density and other artefacts in the peat (Belcher et al., 2010; Frandsen, 1987; Hadden et al., 2013; Zaccone et al., 2014). We note that studying smouldering fire behaviour in field samples of peat soil would make the analysis more complex and the results more difficult to interpret because of the multiple uncontrolled factors (e.g. bulk density, organic composition, pore size) that vary between field samples (McMahon et al., 1980). Our results (Prat-Guitart et al., 2016) and those of others indicate that the spread of smouldering fire in natural peats will also be influenced by peat bulk density (Frandsen, 1991; Lukenbach et al., 2015), mineral content (Frandsen, 1987; Garlough and Keyes, 2011), depth (Benscoter et al., 2011; Huang and Rein, 2015), as well as the organic composition, structure, pore size distribution and the degree of decomposition. Future research should aim to further develop our experimental work to understand

how other peat properties contributing to the heterogeneity of moisture content of peatlands affect the spread of peat fires.

4.2. Application to peatland fires

The results obtained in our milled peat experiments in the laboratory where a moisture content gradient was implemented for the first time, give a first insight to the understanding of the peat fire behaviour and interpretation of post peat-fire landscapes. Often, post fire studies report irregular consumption of peat, where wet *Sphagnum* hummocks are left unburnt (Benscoter and Wieder, 2003; Hudspith et al., 2014; Shetler et al., 2008). Our results suggest that differences in peat moisture content could cause smouldering consumption in the dry peat surrounding *Sphagnum* hummocks and likely reduced the size of the wet patches.

In peatlands, smouldering fires happen during extreme weather events, due to reductions of surface moisture content (Terrier et al., 2014; Turetsky et al., 2015). Peat fires in surface peat layers are part of the natural cycle of peatlands, often limited by the spatial heterogeneity of moisture content. These fires reduce peat accumulation, enhance biodiversity and facilitate the access of surface vegetation to the water table (Waddington et al., 2015). The spatial distribution of moisture content at a microtopographical scale has a strong influence on the smouldering fire spread (Benscoter and Wieder, 2003). We predicted fire spread of <10 cm into a wet patch for most of the moisture content combinations involving peat ≥ 160% *MC* (Fig. 7). *Sphagnum* hummocks have a variable size, between 20 and 200 cm diameter (Nungesser, 2003; Petrone et al., 2004), meaning than most of the hummock surface can remain unburnt. Natural peatlands have high water table levels and heterogeneous distributions of surface moisture (Waddington et al., 2015). Our controlled peat experiments have only looked at surface horizontal spread. This is one kind of spread that, together with vertical spread, happens during peat fires due to the three-dimensional shape of the smouldering front (Ohlemiller, 2002). Future modelling of peatland fires needs to consider variations in the underlying moisture content because of its effect on the smouldering propagation at a fine-scale in more complex smouldering spread scenarios. Modelling of peat fires incorporating the effect of peat moisture changes will lead to more accurate estimates of carbon emissions, fire perimeter and area burned (Benscoter and Wieder, 2003). Finally, ecosystem management and fire management should also take into account the spatial variation of peat moisture content to manage the fire risk, avoid large areas of peat being consumed by fires and moisture maps may allow better estimates of fire or burn severity to be made. It may be that peat fires can be managed by assuming that extinction could be achieved by rising the moisture content of strategically located peat areas above 200% *MC*. This technique may have a wider range of ecological benefits than flooding entire areas by blocking ditches or using destructive techniques such as bull-dozing trenches (Davies et al., 2013; Watts, 2012).

5. Conclusions

We studied the role of moisture content as a limiting factor of smouldering propagation in situations where peat moisture content is not homogeneous. Our approach presents a useful method toward building an understanding peatland smouldering fire behaviour that enable new information about the influence of moisture content transitions in peatland systems. We show that fire spread into wet peat patches is strongly affected by local transitions of moisture content. The moisture content of the peat before the transition governs the fire behaviour into a wet peat for the first centimetres of spread. After that distance it is likely that peat fires self-extinguish leaving unburnt patches of wet peat. Future research on peat fire behaviour should consider local variation in moisture content to better understand the spread of smouldering fronts through peat layers.

Acknowledgements

The authors thank the School of Mechanical Engineering at University College Dublin, especially to David Timoney for the support and John Gahan for his help during the laboratory set up. We thank M. Waddington and one anonymous reviewer that provided helpful comments on the manuscript. This project is funded by the Irish Higher Education Authority PRLTI 5. Claire M. Belcher acknowledges a European Research Council Starter Grant ERC-2013-StG-335891-ECOFLAM.

Appendix A. Supplementary data

Supplementary data to this article can be found online at http://dx.doi.org/10.1016/j.scitotenv.2016.02.145.

References

Belcher, C.M., Yearsley, J.M., Hadden, R.M., McElwain, J.C., Rein, G., 2010. Baseline intrinsic flammability of Earth's ecosystems estimated from paleoatmospheric oxygen over the past 350 million years. Proc. Natl. Acad. Sci. 107, 22448–22453.
Benscoter, B.W., Wieder, R.K., 2003. Variability in organic matter lost by combustion in a boreal bog during the 2001 Chisholm fire. Can. J. For. Res. 33, 2509–2513.
Benscoter, B.W., Thompson, D.K., Waddington, J.M., Flannigan, M.D., Wotton, B.M., de Groot, W.J., Turetsky, M.R., 2011. Interactive effects of vegetation, soil moisture and bulk density on depth of burning of thick organic soils. Int. J. Wildland Fire 20, 418–429.
Billett, M.F., Charman, D.J., Clark, J.M., Evans, C.D., Evans, M.G., Ostle, N.J., Worrall, F., Burden, A., Dinsmore, K.J., Jones, T., McNamara, N.P., Parry, L., Rowson, J.G., Rose, R., 2010. Carbon balance of UK peatlands: current state of knowledge and future research challenges. Clim. Res. 45, 13–29.
Bivand, R.S., Pebesma, E.J., Gomez-Rubio, V., 2008. Applied Statistical Data Analysis With R. Springer-Verlag, Berlin Heidelberg.
Boelter, D.H., 1965. Hydraulic conductivity of peats. Soil Sci. 100, 227–231.
Chen, H., Zhao, W., Liu, N., 2011. Thermal analysis and decomposition kinetics of Chinese forest peat under nitrogen and air atmospheres. Energy Fuel 25, 797–803.
Crawley, M.J., 2013. The R Book. John Wiley and Sons Ltd, West Sussex.
Davies, G.M., Gray, A., Rein, G., Legg, C.J., 2013. Peat consumption and carbon loss due to smouldering wildfire in a temperate peatland. For. Ecol. Manag. 308, 169–177.
Developement Core Team, 2013. R: A Language and Environment for Statistical Computing.
Flannigan, M.D., Stocks, B., Turetsky, M.R., Wotton, B.M., 2009. Impacts of climate change on fire activity and fire management in the circumboreal forest. Glob. Chang. Biol. 15, 549–560.
Frandsen, W.H., 1987. The influence of moisture and mineral soil on the combustion limits of smouldering forest duff. Can. J. For. Res. 17, 1540–1554.
Frandsen, W.H., 1991. Burning rate of smouldering peat. Northwest Sci. 65, 166–172.
Frandsen, W.H., 1997. Ignition probability of organic soils. Can. J. For. Res. 27, 1471–1477.
Garlough, E.C., Keyes, C.R., 2011. Influences of moisture content, mineral content and bulk density on smouldering combustion of ponderosa pine duff mounds. Int. J. Wildland Fire 20, 589–596.
Gorham, E., 1991. Northern peatlands: role in the carbon cycle and probable responses to climate warming. Ecol. Appl. 1, 182–195.
Hadden, R.M., Rein, G., Belcher, C.M., 2013. Study of the competing chemical reactions in the initiation and spread of smouldering combustion in peat. Proc. Combust. Inst. 34, 2547–2553.
Hayward, P.M., Clymo, R.S., 1982. Profiles of water content and pore size in *Sphagnum* and peat, and their relation to peat bog ecology. Proc. R. Soc. B Biol. Sci. 215, 299–325.
Hiemstra, P.H., Pebesma, E.J., Twenhofel, C.J.W., Heuvelink, G.B.M., 2009. Real-time automatic interpolation of ambient gamma dose rates from the Dutch Radioactivity Monitoring Network. Comput. Geosci. 35, 1711–1721.
Hillel, D., 1980. Fundamentals of Soil Physics. Academic Press, London.
Holden, N.M., Ward, S.M., 1997. The physical properties of stockpiled milled peat from midland production bogs. Ir. J. Agric. Food Res. 36, 205–218.
Huang, X., Rein, G., 2014. Smouldering combustion of peat: inverse modelling of the drying and the thermal and oxidative decomposition kinetics. Combust. Flame 161, 1633–1644.
Huang, X., Rein, G., 2015. Computational study of critical moisture and depth of Burn in peat fires. Int. J. Wildland Fire 24, 798–808.
Hudspith, V.A., Belcher, C.M., Yearsley, J.M., 2014. Charring temperatures are driven by the fuel types burned in a peatland wildfire. Front. Plant Sci. 5, 1–12.
IPCC, Climate Change, 2013. The physical science basis. Contribution of Working Group I to the Fifth Assessment Report of the Intergovernmental Panel of Climate Change. Cambridge University Press, Cambridge, United Kingdom and New York, NY, USA.
Kettridge, N., Thompson, D.K., Waddington, J.M., 2012. Impact of wildfire on the thermal behavior of northern peatlands: observations and model simulations. J. Geophys. Res. Biogeosci. 117, 1–14.
Kettridge, N., Humphrey, R.E., Smith, J.E., Lukenbach, M.C., Devito, K.J., Petrone, R.M., Waddington, J.M., 2014. Burned and unburned peat water repellency: implications for peatland evaporation following wildfire. J. Hydrol. 513, 335–341.

Lawson, B.D., Frandsen, W.H., Hawkes, B.C., Dalrymple, G.N., 1997. Probability of Sustained Smouldering Ignition for Some Boreal Forest Duff Types. Nat. Resour. Can., Can. For. Serv., North. For. Cent., Edmonton, Alberta, p. 63.

Lukenbach, M.C., Hokanson, K.J., Moore, P.A., Devito, K.J., Kettridge, N., Thompson, D.K., Wotton, B.M., Petrone, R.M., Waddington, J.M., 2015. Hydrological controls on deep burning in a northern forested peatland. Hydrol. Process. 29, 4114–4124.

Mack, M.C., Bret-Harte, M.S., Hollingsworth, T.N., Jandt, R.R., Schuur, E.A.G., Shaver, G.R., Verbyla, D.L., 2011. Carbon loss from an unprecedented Artic tundra wildfire. Nature 475, 489–492.

McCarter, C.P.R., Price, J.S., 2012. Ecohydrology of *Sphagnum* moss hummocks: mechanisms of capitula water supply and simulated effects of evaporation. Ecohydrology 7, 33–44.

McMahon, C., Wade, D., Tsoukalas, S., 1980. Combustion characteristics and emissions from burning organic soils. Proceedings of the 73rd Annual Meeting of the Air Pollution Control Association. Proceedings for the Tall Timbers Fire Ecology Conference, Montreal, QC Paper No. 80–15.5.

Miyanishi, K., Johnson, E.A., 2002. Process and patters of duff consumption in the mixedwood boreal forest. Can. J. For. Res. 32, 1285–1295.

Nungesser, M.K., 2003. Modelling microtopography in boreal peatlands: hummocks and hollows. Ecol. Model. 165, 175–207.

Ohlemiller, T.J., 1985. Modeling of smouderling combustion propagation. Prog. Energy Combust. Sci. 11, 277–310.

Ohlemiller, T.J., 2002. Smoldering combustion. In: DiNeeno, P.J., Drysdale, D., Beyler, C.L., Walton, W.D. (Eds.), SFPE Handbook of Fire Protection Engineering, pp. 200–210.

Page, S.E., Siegert, F., Rieley, J.O., Boehm, H.-D.V., Jaya, A., Limin, S., 2002. The amount of carbon released from peat and forest fires in Indonesia during 1997. Nature 420, 61–65.

Pebesma, E.J., 2004. Multivariable geostatistics in S: the gstat package. Comput. Geosci. 30, 683–691.

Petrone, R.M., Price, J.S., Carey, S.K., Waddington, J.M., 2004. Statistical characterization of the spatial variability of soil moisture in a cutover peatland. Hydrol. Process. 18, 41–52.

Prat-Guitart, N., Hadden, R.M., Belcher, C.M., Rein, G., Yearsley, J.M., 2015. Infrared image analysis as a tool for studying the horizontal smoldering propagation of laboratory peat fires. In: Stracher, G.B., Prakash, A., Rein, G. (Eds.), Coal and Peat Fires, A Global PerspectivePeat — Geology, Combustion and Case Studies. Elsevier, Amsterdam, pp. 121–139.

Prat-Guitart, N., Rein, G., Hadden, R.M., Belcher, C.M., Yearsley, J.M., 2016. Propagation probability and spread rates of self-sustained smouldering fires under controlled moisture content and bulk density conditions. Int. J, Wildland Fire http://dx.doi.org/10.1071/WF15103.

Putzeys, O., Bar-Ilan, A., Rein, G., Fernandez-Pello, A.C., Urban, D.L., 2007. The role of secondary char oxidation in the transition from smoldering to flaming. Proc. Combust. Inst. 31, 2669–2676.

Reardon, A.J., Hungerford, R., Ryan, K.C., 2007. Factors affecting sustained smouldering in organic soils from pocosin and pond pine woodland wetlands. Int. J. Wildland Fire 16, 107–118.

Rein, G., 2013. Smouldering fires and natural fuels. In: CM, Belcher (Ed.), Fire Phenomena in the Earth System. An Interdisciplinary Approach to Fire Science. Wiley-Blackwell, pp. 15–34.

Rein, G., 2016. Smouldering combustion. In: Hurley, M.J., Gottuk, D.T., Hall Jr., J.R., Harada, K., Kuligowski, E.D., Puchovsky, M., Torero, J.L., Watts Jr., J.M., Wieczorek, C.J. (Eds.), SFPE Handbook of Fire Protection Engineering SE-19. Springer, New York, pp. 581–603.

Rein, G., Cleaver, N., Ashton, C., Pironi, P., Torero, J.L., 2008. The severity of smouldering peat fires and damage to the forest soil. Catena 74, 304–309.

Roulet, N., Moore, T., Bublier, J., Lafleur, P., 1992. Northern fens: methane flux and climate change. Tellus 44B, 100–105.

Shetler, G., Turetsky, M.R., Kane, E.S., Kasischke, E.S., 2008. Sphagnum mosses limit total carbon consumption during fire in Alaskan black spruce forests. Can. J. For. Res. 38, 2328–2336.

Terrier, A., Groot, W.J., Girardin, M.P., 2014. Dynamics of moisture content in spruce–feather moss and spruce–*Sphagnum* organic layers during an extreme fire season and implications for future depths of burn in Clay Belt black spruce forests. Int. J. Wildland Fire 23, 490–502.

Thompson, D.K., Waddington, J.M., 2013. Peat properties and water retention in boreal forested peatlands subject to wildfire. Water Resour. Res. 49, 3651–3658.

Turetsky, M.R., Wieder, K., Halsey, L., Vitt, D., 2002. Current disturbance and the diminishing peatland carbon sink. Geophys. Res. Lett. 29, 7–10.

Turetsky, M.R., Donahue, W.F., Benscoter, B.W., 2011. Experimental drying intensifies burning and carbon losses in a northern peatland. Nat. Commun. 2, 514.

Turetsky, M.R., Benscoter, B., Page, S., Rein, G., van der Werf, G.R., Watts, A., 2015. Global vulnerability of peatlands to fire and carbon loss. Nat. Geosci. 8, 11–14.

Waddington, J.M., Morris, P.J., Kettridge, N., Granath, G., Thompson, D.K., Moore, P.A., 2015. Hydrological feedbacks in northern peatlands. Ecohydrology 8, 113–127.

Watts, A., 2012. Organic soil combustion in cypress swamps: moisture effects and landscape implications for carbon release. For. Ecol. Manag. 294, 178–187.

Wellock, M.L., Reidy, B., Laperle, C.M., Bolger, T., Kiely, G., 2011. Soil organic carbon stocks of afforested peatlands in Ireland. Forestry 84, 441–451.

Yu, Z.C., 2012. Northern peatland carbon stocks and dynamics: a review. Biogeosciences 9, 4071–4485.

Zaccone, C., Rein, G., D'Orazio, V., Hadden, R.M., Belcher, C.M., Miano, T.M., D'Orazio, V., Hadden, R.M., Belcher, C.M., Miano, T.M., 2014. Smouldering fire signatures in peat and their implications for palaeoenvironmental reconstructions. Geochim. Cosmochim. Acta 137, 134–146.